

## Temperature-Dependent Electric Quadrupole Interaction of $^{67}\text{Zn}$ in Zinc Metal

H. Bertschat\*, E. Recknagel, and B. Spellmeyer

*Bereich Kern- und Strahlenphysik, Hahn-Meitner-Institut für Kernforschung Berlin, Berlin-West, Germany,  
and Fachbereich Physik der Freien Universität, Berlin-West, Germany*

(Received 15 November 1973)

By means of time-differential observation of perturbed angular distributions of  $\gamma$  radiation following the nuclear reaction  $^{66}\text{Zn}(d, p)$ , the electric quadrupole interaction frequency of the isomeric  $\frac{5}{2}^+$  state of  $^{67}\text{Zn}$  in zinc metal has been measured as a function of temperature. At room temperature the frequency was determined to be  $e^2qQ/\hbar = 45.5(4)$  MHz. The temperature dependence is compared with previous results for  $^{111}\text{Cd}$  in cadmium.

We have investigated the electric quadrupole interaction of  $^{67m}\text{Zn}$  in zinc. The aim of the experiment was to study the temperature dependence of the electric field gradient (EFG) in this hcp metal, and to estimate the quadrupole moment of the excited  $\frac{5}{2}^+$  state of  $^{67}\text{Zn}$  ( $E = 605$  keV,  $T_{1/2} = 333$  nsec), which was used as the probe nucleus. The measurement was performed by time-differential observation of perturbed angular distributions of  $\gamma$  radiation following the nuclear reaction  $^{66}\text{Zn}(d, p)$ .

Recently, several investigations of the electric quadrupole interaction in cadmium, which is the second hcp metal of the IIB group, have been reported.<sup>1-5</sup> Using the isomeric  $\frac{5}{2}^+$  state of  $^{111}\text{Cd}$  as a probe, some of them<sup>1-3</sup> were carried out by the time-differential perturbed angular correlation method with radioactive sources, while two of them<sup>4,5</sup> were performed via recoil implantation techniques, which additionally yield information about relaxation effects caused by radiation damage. The quadrupole interaction, which can be influenced by the measurement process, was found to have the same strength with both methods except for the low-temperature region, where radiation-damage effects cause slight differences.<sup>5</sup> The variation of the quadrupole interaction frequency with temperature has been found to be a strong effect. However, no explanation of the temperature dependence of the Cd EFG has been presented up to now. An extension of these measurements to zinc should be useful for a better understanding of the EFG's in hcp metals.

A pulsed deuteron beam of the 7-MV Van de Graaff accelerator of the Hahn-Meitner-Institut Berlin was used to populate the  $\frac{5}{2}^+$  state of  $^{67}\text{Zn}$  (pulse width  $\Delta t = 10$  nsec, repetition time  $T = 2$   $\mu\text{sec}$ , deuteron energy  $E = 6.4$  MeV, deuteron current  $i = 30$  nA). The target, an isotopically enriched (99%) polycrystalline  $^{66}\text{Zn}$  metal disk

of about 30 mg, was mounted on a metal finger, which could be heated electrically to temperatures between 300 K and the melting point. The temperature was measured by a thermocouple. The target was fixed in a chamber, which was separated from the accelerator vacuum system by a thin Havar foil. A hydrogen gas stream, at a pressure of about 100 Torr, flowed through the chamber to prevent oxidation of the zinc surface. The  $\gamma$  radiation was detected by two  $2 \times 1.5$  in.<sup>2</sup> NaI(Tl) scintillators arranged at angles  $\theta = 0^\circ$  and  $90^\circ$  with respect to the beam axis.

The time-dependent  $\gamma$ -ray distribution is described by<sup>6</sup>  $W(\theta, t) = 1 + A_2 G_2(t) P_2(\cos \theta)$ , neglecting terms with  $k > 2$ . The modulation amplitude

$$G_2(t) = \sum_{n=0}^7 s_{2n} \cos(n\omega_0 t)$$

is the spin-dependent perturbation factor for an axially symmetric field gradient in a microcrystal; it is a function of the basic modulation frequency  $\omega_0 = e^2qQ/24\hbar$ . After removal of the nuclear decay factor  $e^{-\lambda t}$ , the experimental time-distribution patterns were analyzed by least-squares fits of the difference of the counting rates:

$$\frac{2}{3} [W(0^\circ, t) - W(90^\circ, t)] = A_2 G_2(t).$$

The spin precession spectra for different temperatures and their fits are shown in Fig. 1.

Before we discuss the experimental results some remarks concerning the final positions of the probe nuclei and their surroundings should be made. There exists evidence from in-beam experiments<sup>4,5,7</sup> that a high percentage of recoiling nuclei reach substitutional lattice sites, probably by replacement collisions, within the experimentally unresolved time interval after the beam pulse. This is confirmed in our experiment by the fact that each spectrum, even the measure-

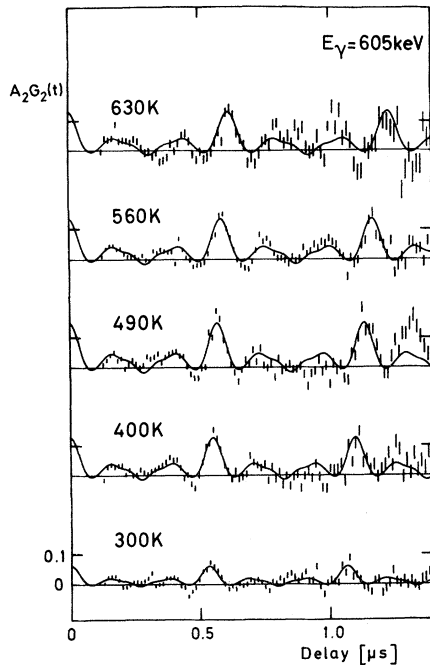


FIG. 1. Time-differential perturbed angular-distribution spectra of  $^{67}\text{Zn}(\frac{5}{2}^+)$  in polycrystalline zinc metal for different temperatures. The solid curves are least-squares fits, assuming EFG's with axial symmetry.

ment at 300 K, could be fitted assuming a sharp frequency; we may therefore assume that in each case the excited nuclei experience a unique EFG. Furthermore, in the temperature region above 400 K no significant damping of the modulation amplitude was observed, and hence one can exclude possible radiation-damage effects such as vacancies or interstitials in the immediate surroundings of the probe nucleus, which

could lead to frequency distributions. Only in the measurement at room temperature does the perturbation amplitude appear to be strongly reduced within the first 50 nsec after the beam pulse. This appears to indicate that the dynamic process causing such a relaxation of the nuclear alignment takes place during the (temperature-dependent) time interval which is required for the regeneration of the surrounding lattice after the stopping process. There are, however, some unexplained deviations from the theoretical curves. As they cannot be fitted by the introduction of an asymmetry parameter  $\eta = (q_{xx} - q_{yy})/q_{zz}$ , we see no reason to revise the original assumption of axial symmetry for the EFG.

In Table I the experimental results are summarized. The data are analyzed under the following aspects: (1) determination of the quadrupole interaction frequency and estimate of the quadrupole moment, (2) temperature dependence of the interaction frequency.

(1) The spin of the isomeric state can be deduced from the spin rotation pattern to be  $I = \frac{5}{2}$  in agreement with a previous  $(d, p)$  reaction experiment,<sup>8</sup> and the measurement of the magnetic moment.<sup>9</sup> The quadrupole interaction frequency, graphically extrapolated to  $T = 0$  K, is  $e^2qQ/h = 49.5(15)$  MHz. However, no reliable determination of the electric quadrupole moment is possible because of the unknown EFG in zinc. A very rough indication of the strength of the EFG can be taken from investigations of the quadrupole interaction of impurities in zinc and cadmium<sup>3</sup> which lead to the same EFG's for both metals within an accuracy of about 30%. Therefore, taking the quadrupole moment of the excited  $\frac{5}{2}^+$  state of  $^{111}\text{Cd}$  to be  $|Q| = 0.5$  b, given also

TABLE I. Experimental results and semiempirical calculations.

Temperature (K)	Perturbation amplitude <sup>a</sup>	$e^2qQ/h$ (MHz)	$eq_{\text{lat}}^b$ ( $10^{13}$ esu/cm <sup>3</sup> )	$eq_{\text{el}}^c$
300(10)	0.063(7)	45.5(4)	-49.3	363
400(10)	0.127(10)	44.0(3)	-51.2	354
490(15)	0.147(13)	42.6(3)	-52.5	346
560(15)	0.138(9)	41.4(3)	-53.5	339
630(15)	0.133(13)	39.3(4)	-54.3	325

<sup>a</sup>  $A_2G_2(t)$  at  $t = 2\pi N/\omega_0$ .

<sup>b</sup> Calculated using the formula  $q_{\text{lat}} = 2(1 + \gamma_\infty)[0.0065 - 4.3584(c/a - 1.633)] \times a^{-3}$  (Refs. 11, 13).

<sup>c</sup>  $q_{\text{el}} = q_{\text{exp}} - q_{\text{lat}}$ , calculated under the assumption  $|Q(\text{Zn})| = 0.2$  b; the values for  $q_{\text{exp}}$  were taken from the smoothed experimental curve A in Fig. 2.

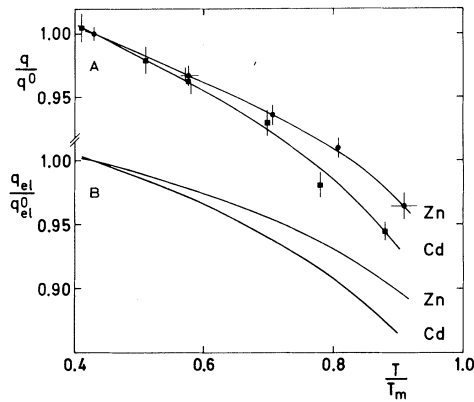


FIG. 2. A, temperature dependence of the experimentally determined EFG in reduced coordinates. The values for Cd are taken from Ref. 5. The solid lines are hand drawn. B, temperature dependence of the semiempirically obtained conduction-electron contribution (see text).

in Ref. 3, we obtain from the ratio of the quadrupole interaction frequencies of  $^{111}\text{Cd}$  (137.5 MHz)<sup>1</sup> and  $^{67}\text{Zn}$  (49.5 MHz) at 0 K the value  $|Q| = 0.18$  b for the quadrupole moment of  $^{67}\text{Zn}$ . This value can be wrong by a factor of 2, which is mainly due to the large uncertainty of the Cd moment. A calculation of the Zn moment using the core polarization theory<sup>10</sup> yields a value of  $Q = 0.2$  b.

(2) The temperature dependence of the quadrupole interaction frequency, i.e., of the EFG, observed by the  $^{67}\text{Zn}$  probe in zinc, together with the values for  $^{111}\text{Cd}$  in cadmium (taken from Ref. 5), is plotted in Fig. 2, curves A. For comparison the coordinates are reduced, using for arbitrary normalization the melting temperatures [ $T_m(\text{Zn}) = 693$  K,  $T_m(\text{Cd}) = 594$  K] and the interaction frequencies at  $T/T_m = 0.432$ , i.e., 300 K for Zn and 257 K for Cd. The solid lines are drawn by hand to smooth the experimental values. Both curves show a similar behavior, though the temperature dependence of the EFG in zinc is less pronounced.

We briefly turn to discuss the theoretical attempts to calculate the EFG's of metals. It has become usual to attribute the EFG to two main sources, namely, the lattice contribution  $q_{\text{lat}}$  and the conduction-electron contribution  $q_{\text{el}}$ , so that  $q \approx q_{\text{lat}} + q_{\text{el}}$ . While the lattice contribution can be calculated by straightforward summation over the ionic sites of the crystal,<sup>11</sup> the conduction-electron part requires a detailed scanning of the occupied Fermi volume. Recently,<sup>12</sup> an evaluation of  $q_{\text{el}}$  at  $T = 0$  K has been reported for cadmium,

using the pseudopotential approximation for obtaining the energy bands and band wave functions in the entire Fermi volume. As an important result of that work the sign of  $q_{\text{el}}$  was found to be positive, opposite to that of  $q_{\text{lat}}$ . Up to now, no similar treatment exists for zinc. We therefore calculated only the lattice contribution  $q_{\text{lat}}$  from the lattice parameters  $c/a$  and  $a$ , varying with temperature.<sup>11,13</sup> The results are given in column 4 of Table I. With the aid of these values and the estimated quadrupole moment, the semiempirical values for  $eq_{\text{el}}$ , shown in column 5, are derived. The sign of  $e^2qQ/\hbar$  was assumed to be positive in order to obtain a positive sign for  $eq_{\text{el}}$ , in analogy to the cadmium case. We find the ratio  $|q_{\text{lat}}/q_{\text{el}}| \approx 1/7$  at  $T/T_m = 0.43$ . The same calculation for cadmium<sup>13</sup> with  $|Q(\text{Cd})| = 0.5$  b (Ref. 3) yields for the absolute value of this ratio the value  $1/6.5$ .

The normalized conduction-electron contribution is plotted in Fig. 2, curves B. From this semiempirical treatment it can be seen that the temperature behavior of the EFG is mainly governed by the conduction-electron part, slightly enhanced by the lattice contribution. This result remains valid if the considerable uncertainties of the quadrupole moments are taken into account. Furthermore, it turns out that it is also the conduction-electron contribution which is mainly responsible for the discrepancy between Zn and Cd.

We thank H. Haas, U. Leithäuser, and K. H. Maier for helpful discussions and their assistance during the measurement. We gratefully acknowledge financial support by the Bundesministerium für Wissenschaft und Technologie.

\*Work performed in partial fulfillment of the requirements for a doctorate in science.

<sup>1</sup>R. S. Raghavan and P. Raghavan, Phys. Lett. **36A**, 313 (1971).

<sup>2</sup>E. Bodenstedt, U. Ortabasi, and W. H. Ellis, Phys. Rev. B **6**, 2909 (1972).

<sup>3</sup>H. Haas and D. A. Shirley, J. Chem. Phys. **58**, 3339 (1973).

<sup>4</sup>J. M. McDonald, P. M. S. Lesser, and D. B. Fossan, Phys. Rev. Lett. **28**, 1057 (1972).

<sup>5</sup>J. Bleck, R. Butt, H. Haas, W. Ribbe, and W. Zeitz, Phys. Rev. Lett. **29**, 1371 (1972).

<sup>6</sup>H. Frauenfelder and R. M. Steffen, in *Alpha-, Beta-, and Gamma-Ray Spectroscopy*, edited by K. Siegbahn (North-Holland, Amsterdam, 1965), Vol. 2, p. 997.

<sup>7</sup>H. Haas, W. Leitz, H.-E. Mahnke, W. Semmler, R. Sielemann, and Th. Wichert, Phys. Rev. Lett. **30**, 656 (1973).

<sup>8</sup>D. von Ehrenstein and J. P. Schiffer, Phys. Rev. **164**, 1374 (1967).

<sup>9</sup>H. Bertschat, U. Leithäuser, K. H. Maier, E. Recknagel, and B. Spellmeyer, to be published.

<sup>10</sup>H. Noya, A. Arima, and H. Horie, Progr. Theor. Phys., Suppl. No. 8, 33 (1958).

<sup>11</sup>T. P. Das and M. Pomerantz, Phys. Rev. **123**, 2070 (1961).

<sup>12</sup>N. C. Mohapatra, C. M. Singal, and T. P. Das, Phys. Rev. Lett. **31**, 580 (1973).

<sup>13</sup>Interpolated lattice parameters for Zn: *Gmelins Handbuch der anorganischen chemie, Zink, Ergänzungsband* (Verlag Chemie, Weinheim, Germany, 1956), p. 282. Interpolated lattice parameters for Cd: *ibid.*, *Cadmium, Ergänzungsband* (Verlag Chemie, Weinheim, Germany, 1959), p. 56.

## Electroproduction of $K^+$ Mesons in the Forward Direction\*

C. J. Bebek, C. N. Brown, M. Herzlinger, S. Holmes, C. A. Lichtenstein, F. M. Pipkin,  
and L. K. Sisterson

*Cyclotron Laboratory, Harvard University, Cambridge, Massachusetts 02138*

and

D. Andrews,† K. Berkelman, D. G. Cassel, and D. L. Hartill  
*Laboratory of Nuclear Studies, Cornell University, Ithaca, New York 14850*

and

N. Hicks

*Wellesley College, Wellesley, Massachusetts 02181*

(Received 23 October 1973)

We present data on electroproduction of  $K^+$  mesons off protons. Measurements were made at data points with nominal  $(Q^2, W)$  values of (0.6, 2.67), (1.2, 2.67), (2.0, 2.67), and (1.2, 2.15) in  $(\text{GeV}^2, \text{GeV})$ . The virtual photoproduction cross section for  $K^+ + \text{MM}$  is studied as a function of missing mass,  $x'$ ,  $P_{\perp}^2$ ,  $Q^2$ , and  $W$ . The data show that the  $K^+\Sigma^0$  cross section falls more rapidly than the  $K^+\Lambda^0$  cross section as  $Q^2$  increases.

This paper reports measurements made at the Wilson Synchrotron Laboratory of the electroproduction of  $K^+$  mesons from a proton target.

In what is now standard notation,<sup>1</sup> electroproduction is treated as photoproduction by a virtual photon. The square of the proton's mass  $-Q^2$ , energy  $\nu$ , direction, and polarization  $\epsilon$  are tagged by the scattered electron. The hadronic cross section is a function of the virtual-photon variables and the variables describing the produced hadron in the virtual-photon-proton center-of-mass system,  $\theta^*$ ,  $\varphi$ , and  $(\text{MM})^2$ . The virtual photoproduction cross section can also be written in terms of the scaling variables  $x'$  and  $P_{\perp}^2$  defined in Bebek *et al.*<sup>2</sup> We have analyzed the inclusive data in terms of the cross-section differential in  $(\text{MM})^2$  and of the invariant structure function

$$F = \frac{E}{\sigma_{\text{tot}}} \frac{d^3\sigma}{dp^3} = \frac{1}{\sigma_{\text{tot}}} \frac{1}{\pi} \frac{E^*}{[P_{\text{max}}^{*2} - P_{\perp}^2]^{1/2}} \frac{d\sigma}{dx' dP_{\perp}^2}$$

Here  $\sigma_{\text{tot}}$  is the total virtual photoproduction cross section for the total energy  $W$  and  $Q^2$  of the

reaction. The value of  $\sigma_{\text{tot}}$  was taken from a fit to the Stanford Linear Accelerator Center-Massachusetts Institute of Technology measurements of  $\nu W_2$  made with the assumption  $\sigma_s/\sigma_T = 0.18$ .<sup>3</sup>

Two magnetic spectrometers were used to detect the scattered electron and the electroproduced hadron. The combination of a Cherenkov counter and a lead-acetate shower counter identified the electrons. Pions were identified by a threshold gas Cherenkov counter when their momentum was greater than 1.8 GeV/c and by their time of flight when their momentum was less than that. Kaons were separated from protons by their time of flight.

Data were taken at the points in the  $(Q^2, \nu)$  plane shown in Fig. 1. Points 1, 3, and 7 comprise a  $Q^2$  scan at fixed  $W$ ; points 6 and 7 lie on the same  $\omega$  line and give a test of scaling; points 3 and 6 give a  $W$  scan at fixed  $Q^2$ ; and points 2, 4, and 5 give an angular scan with the hadron arm which extends the aperture in  $P_{\perp}$ . The acceptance of the apparatus is such that at each datum point the  $W$  distribution is approximately 0.6 GeV wide and